Int. J. Solids Structures Vol. 29, No. 16, pp. 2091–2100, 1992
Printed in Great Britain.

0020–7683/92 $5.00 + .00

UNI-DIRECTIONAL BUCKLING OF A PINNED ELASTICA WITH EXTERNAL PRESSURE

R. H. PLAUT
Charles E. Via, Jr. Department of Civil Engineering, Virginia Polytechnic Institute and State University, Blacksburg, VA 24061, U.S.A.

and

Z. MRÓZ
Institute of Fundamental Technological Research, Polish Academy of Sciences, Swietokrzyska 21, PL 00-049 Warsaw, Poland

(*Received* 1 *February* 1991; *in revised form* 1 *November* 1991)

Abstract—Uni-directional buckling of an elastica with pinned ends is investigated. A rigid foundation below the beam prohibits downward deflection, and a uniform pressure acts on the beam from above. The beam weight is neglected, and an axial compressive load is applied. Equilibrium paths are determined for various pressures, and the effects of initial curvature and load eccentricity are examined.

INTRODUCTION

The one-way buckling of an elastica is considered. The beam has pinned ends and is subjected to a compressive load. A rigid foundation lies on one side of the beam and a uniform pressure acts on the other side. The weight of the beam is neglected.

A similar problem was investigated by Wang (1985). In his case, the elastica (or sheet) was long and only a central portion buckled, so that there was no rotation at the points of lift-off from the rigid foundation. Wang only treated the perfect system, whereas the present study includes beams having initial curvature and loads applied eccentrically.

A related problem is that of a compressed horizontal beam lying on a rigid foundation and subjected to a uniformly distributed vertical load, which may represent the weight of the beam [e.g. see Wang (1986) and the references cited therein]. If this system is perfect, buckling does not occur for a finite compressive load (i.e. there is no bifurcation from the flat configuration). However, if the beam is compressed and then disturbed, it may suddenly snap to a buckled shape. Also, if the beam has some initial curvature and is compressed with a quasi-statically increasing load, it may deform continuously for a while and then exhibit the snapping phenomenon. These results may be relevant for the behavior of sheets of paper, textiles, plastics or metals.

Such problems involving transverse resistance occur in a number of fields. One is the buckling of railroad tracks due to compressive loads caused by temperature rises (El-Aini, 1976; Kerr, 1973, 1974, 1976, 1978a, b, 1979, 1980; Tvergaard and Needleman, 1981; Samavedam *et al.*, 1988). Vertical buckling of tracks is similar to that of the heavy beam, but in horizontal (lateral) buckling the mode is not constrained to be uni-directional.

Buckling of pipelines, either buried or lying in trenches or on the seabed, is another related problem (Courbon, 1980; Hobbs, 1981, 1984; Ariman, 1983; Kyriakides *et al.*, 1983; Yun and Kyriakides, 1985, 1986, 1988, 1990; Taylor and Gan, 1986; Ju and Kyriakides, 1988; Nielsen *et al.*, 1988, 1990; Pedersen and Jensen, 1988; Pedersen and Michelsen, 1988; Vinogradov, 1988; Friedmann, 1989; Hobbs and Liang, 1989; Koh and Quek, 1990; and Richards, 1990). For example, the compressive loads may be caused by hot oil or gas in the pipeline, or by ground movement resulting from seismic activity or differential thawing of frozen soil. Roorda (1988) discussed "blow-up" failures of concrete roads and runways and the growth of delaminations in composite laminates, while Hobbs (1989, 1990) treated two-dimensional buckling of heavy plates resting on a rigid plane. Other related

problems are the buckling of floating ice sheets, rock strata (Kerr, 1989), and fibers in composite materials.

In this earlier work, sometimes the displacements are assumed to be small and a linear analysis is carried out, while in other cases geometric nonlinearities are included. If there is a rigid base, it may be frictionless, or frictional resistance to axial displacement may be included, with the friction force sometimes dependent on the tangential deformation. The beams may be either perfectly straight before loading or initially curved. The beam material is usually assumed to be linearly elastic, but nonlinearly elastic and elastic–plastic constitutive laws have also been considered. For a beam surrounded by soil or ballast, the resistance is sometimes taken to be a nonlinear function of the beam displacement, and in some cases of buried pipelines a portion of the buckled shape may protrude out of the soil.

The present paper examines the buckling and post-buckling behavior of a slender, inextensible, uniform, elastic beam [an elastica (Love, 1944)] on a rigid foundation. Deflection of the beam is resisted by a uniform pressure. Compressive axial loads are applied quasi-statically at the ends of the beam, which are simply supported. Two types of imperfection are treated: eccentricity of the axial loads and curvature of the foundation (and beam).

This research is related to work presented in Mróz and Plaut (1992). In that study, buckling and post-buckling behavior of discrete elastic systems lying on a frictional plane are analysed. Resistance to displacement is due to dry friction between the system and the plane. The results obtained here for a pressure resistance are also applicable to the case of such frictional resistance if the friction force has a constant magnitude and only acts in a direction normal to the centerline of the beam.

ELASTICA

Consider the beam shown in Fig. 1. It is inextensible, uniform, slender and elastic with bending stiffness EI. It has length $2L$ and is simply supported at its ends. A rigid foundation lies below the beam, and the beam cannot deflect downward. In Fig. 1(a), the foundation is flat and the unstrained configuration of the beam is flat. In Fig. 1(b), the foundation has some curvature and the unstrained beam has the same curvature and rests on the foundation. The contact between the foundation and the beam is assumed to be frictionless. A buckled configuration is depicted in Fig. 1(c). The horizontal compressive loads are P and the uniform normal force is Q per unit length.

The arc length $\bar{s}$ is measured from the center of the beam. When the beam is unstrained, its configuration is defined by the angle $\theta_0(\bar{s})$ of its tangent (with $\theta_0(\bar{s}) = 0$ if the beam is flat), while $\theta(\bar{s})$ denotes the angle for a deformed configuration. The configurations are assumed to be symmetric about $\bar{s} = 0$, so that $\theta_0(0) = 0$, $\theta(0) = 0$, $\theta_0(-\bar{s}) = -\theta_0(\bar{s})$, and $\theta(-\bar{s}) = -\theta(\bar{s})$. The rotation $\theta(L)$ at the right support is denoted α. The loads P are applied to the ends either at the centerline (i.e. concentrically) or at a small distance Δ normal to the centerline and below it (i.e. eccentrically).

Consider an element of the beam as shown in Fig. 2. The quantities $M(\bar{s})$, $N(\bar{s})$ and $V(\bar{s})$ are the bending moment, axial force and shear force, respectively, with positive senses indicated in Fig. 2. From the equilibrium of tangential forces, moments and normal forces, with $d\bar{s} \to 0$, and from Hooke's law, one obtains the equations

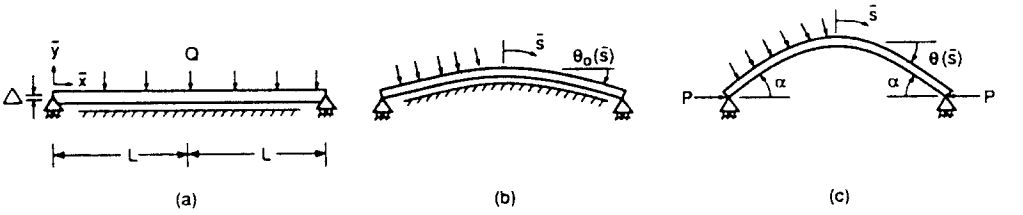

Fig. 1. Geometry of elastica: (a) unbuckled configuration with no initial curvature; (b) unbuckled configuration with initial curvature; (c) buckled configuration.

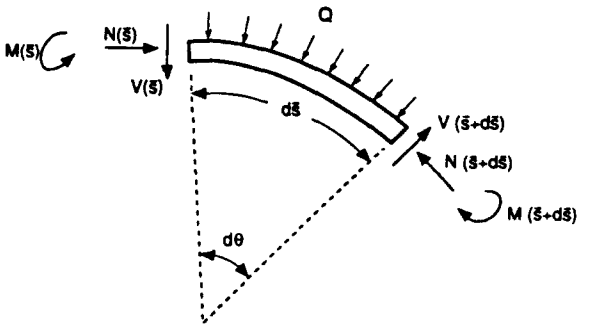

Fig. 2. Equilibrium of element of elastica.

$$N' = V\theta', \quad V = M', \quad V' + N\theta' = Q, \quad M = EI(\theta' - \theta_0'), \qquad (1a, b, c, d)$$

where a prime denotes differentiation with respect to $\bar{s}$.

Assume that the foundation profile and unstrained beam configuration are given by

$$\theta_0(\bar{s}) = \bar{\beta}\bar{s}, \qquad (2)$$

where $\bar{\beta}$ may be zero (flat profile) or a positive constant (circular profile). Then eqns (1a, b, d) lead to the relations

$$V = EI\theta'', \quad N' = EI\theta'\theta''. \qquad (3a, b)$$

Integration of eqn (3b) yields

$$N(\bar{s}) = N_0 + (EI/2)[\theta'(\bar{s})]^2 \qquad (4)$$

where N_0 is a constant. Then substitution of eqns (3a) and (4) into eqn (1c) yields the following nonlinear equation in $\theta(\bar{s})$:

$$EI\theta''' + N_0\theta' + (EI/2)(\theta')^3 = Q. \qquad (5)$$

Since the slope and shear force are zero at the center, and the moment is $P\Delta\cos\alpha$ at the right support, the boundary conditions are

$$\theta(0) = 0, \quad \theta''(0) = 0, \quad EI[\theta'(L) - \theta_0'(L)] = P\Delta\cos\alpha. \qquad (6a, b, c)$$

Also, horizontal equilibrium at $\bar{s} = L$ furnishes the condition

$$P = N_0\cos\alpha + (EI/2)[\theta'(L)]^2\cos\alpha - EI\theta''(L)\sin\alpha \qquad (7)$$

where eqns (3a) and (4) have been used.

Now define the nondimensional quantities

$$s = \bar{s}/L, \quad \gamma^2 = N_0L^2/(EI), \quad p = PL^2/(EI), \quad q = QL^3/(EI), \quad \delta = \Delta/L, \quad \beta = \bar{\beta}L, \qquad (8)$$

and let primes denote differentiation with respect to s. Then eqns (5)–(7) become

$$\theta''' + \gamma^2\theta' + (1/2)(\theta')^3 = q, \qquad \theta(0) = 0, \quad \theta''(0) = 0, \quad \theta'(1) = \beta + p\delta\cos\alpha, \qquad (9, 10)$$

and

$$p = \gamma^2 \cos\alpha + (1/2)[\theta'(1)]^2 \cos\alpha - \theta''(1)\sin\alpha, \tag{11}$$

respectively, while eqn (2) becomes $\theta_0(s) = \beta s$.

In some cases with small curvature θ', a linearized solution will be accurate. Suppose that the term $(1/2)(\theta')^3$ can be neglected in eqn (9). The solution of the resulting linear equation, with boundary conditions (10), is given by

$$\theta(s) = [qs/(\gamma^2)] + [(\beta + \gamma^2\delta)\gamma^2 - q]\sin\gamma s/(\gamma^3\cos\gamma) \tag{12}$$

where $\cos\alpha \approx 1$ has been used when $\delta \neq 0$, and $p = \gamma^2$. This solution becomes unbounded as $\gamma \to \pi/2$, which corresponds to the Euler buckling load $N_0 = \pi^2 EI/(4L^2)$ obtained from the lowest eigenvalue of the linearized system when $q = \beta = \delta = 0$ (a perfect, pinned–pinned column of length $2L$).

PERFECT SYSTEM

In this section, assume that the beam is initially straight ($\beta = 0$) and the load is applied concentrically ($\delta = 0$). Numerical solutions of eqns (9) and (10) are obtained with the use of a shooting method (Wang, 1984). For a specified value of γ^2, eqn (9) is solved by a Runge–Kutta method with "initial conditions" $\theta(0) = 0$, $\theta''(0) = 0$, and different values of $\theta'(0)$ until the condition $\theta'(1) = 0$ is satisfied. Then p is given by eqn (11) with $\alpha = \theta(1)$.

Results are presented in Fig. 3 for nondimensional pressures $q = 0$, 0.1, 0.3, 0.5 and 1.0. The nondimensional compressive load p is plotted as a function of the end rotation α. When there is no pressure ($q = 0$), the nontrivial equilibrium path bifurcates from the trivial solution ($\theta = 0$) at $p = \pi^2/4$. When $q > 0$, there is no bifurcation and the flat beam ($\alpha = 0$) is stable for any load. On the equilibrium paths, $p \to \infty$ as $\alpha \to 0$, and there is a minimum at a value of p larger than $\pi^2/4$. This minimum value of p is called the "safe buckling load" by Kerr (1973) and is $p = 2.68$, 2.84, 2.93 and 3.01 for $q = 0.1$, 0.3, 0.5 and 1.0, respectively. For higher loads, a disturbance may cause the straight elastica to snap suddenly toward the rising (right) side of the equilibrium path in Fig. 3, which is associated with large displacements. Such a jump is sometimes called "upheaval buckling" (Richards, 1990).

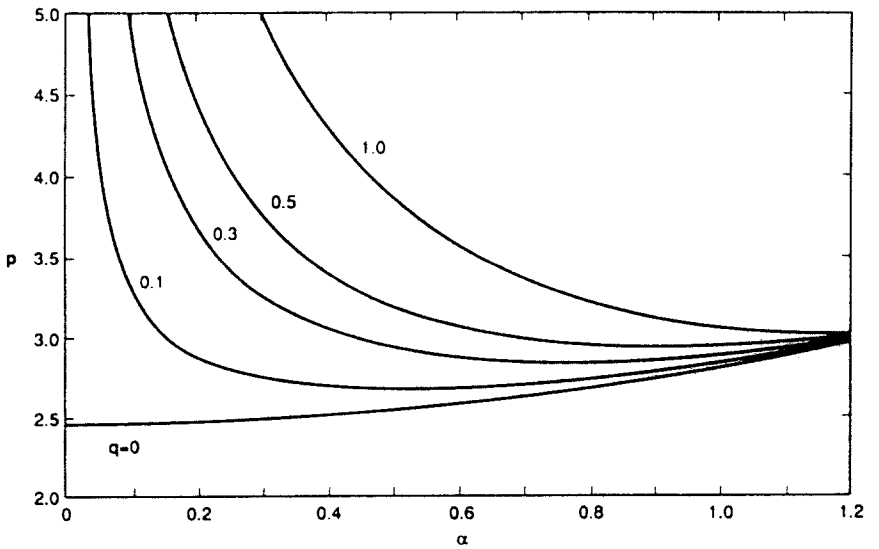

Fig. 3. Effect of pressure on load–displacement curves for elastica; $\beta = 0$, $\delta = 0$.

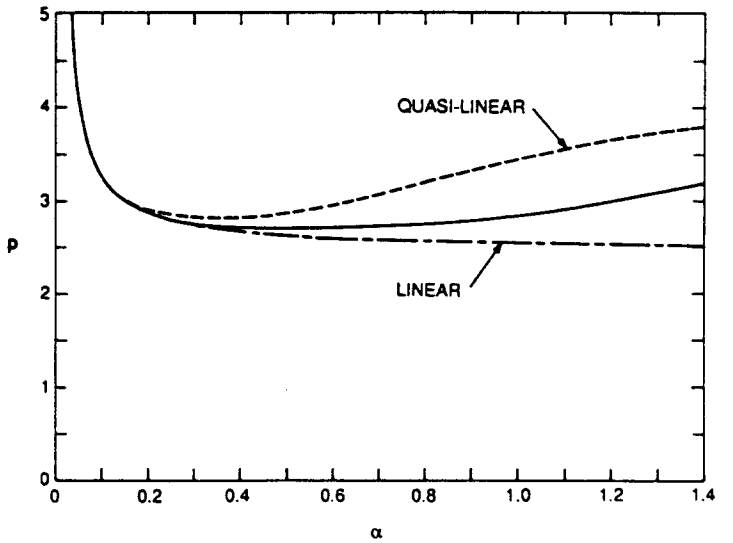

Fig. 4. Load–displacement curves for elastica; $q = 0.1$, $\beta = 0$, $\delta = 0$.

The equilibrium path for $q = 0.1$ is replotted in Fig. 4. In addition, the linear solution is shown as a dash–dot line. It is obtained from eqn (12) with $\beta = \delta = 0$, $\alpha = \theta(1)$, and $p = \gamma^2$, and the equilibrium path decreases monotonically as α increases, approaching the Euler buckling load $p = \pi^2/4$ (Kerr, 1974). If the linear solution (12) is used to determine α, and then the nonlinear relation (11) is applied to obtain p, the resulting pairs (α, p) form the dashed line in Fig. 4, which may be termed a "quasi-linear" solution.

A perturbation analysis was also carried out. For $\beta = \delta = 0$ and small values of q and θ', let

$$q = \sqrt{\varepsilon} r, \quad \theta = \sqrt{\varepsilon}(\psi_1 + \varepsilon\psi_2 + \cdots), \quad \gamma^2 = \gamma_1^2 + \varepsilon\gamma_2^2 + \cdots, \tag{13}$$

where ε is a small parameter. These relations are substituted into eqns (9) and (10), which are then divided by $\sqrt{\varepsilon}$. Setting the coefficients of ε^0 equal to zero yields

$$\psi_1''' + \gamma_1^2\psi_1' = r, \quad \psi_1(0) = \psi_1''(0) = \psi_1'(1) = 0, \tag{14}$$

which has the linear solution (12) with θ replaced by ψ_1, γ by γ_1, and q by r.

Next, the coefficients of ε^1 are set equal to zero. This leads to the system

$$\psi_2''' + \gamma_1^2\psi_2' = -\gamma_2^2\psi_1' - \tfrac{1}{2}(\psi_1')^3, \quad \psi_2(0) = \psi_2''(0) = \psi_2'(1) = 0, \tag{15}$$

which has the solution

$$\psi_2(s) = c_1 s + c_2(\sin\gamma_1 s - \gamma_1 s\cos\gamma_1 s) + c_3\sin 2\gamma_1 s + c_4\sin 3\gamma_1 s \tag{16}$$

where the c_j are given in the Appendix. The functions $\psi_1(s)$ and $\psi_2(s)$ are substituted into eqn (13) to give $\theta(s)$, which can be written in terms of γ_1 and q. The first-order terms (from ψ_1) are proportional to q, and the terms from ψ_2 are proportional to q^3. To obtain numerical results, γ_1 is varied, α is given by $\theta(1)$, and p is determined from eqn (11). For $q = 0.1$, the equilibrium path based on this perturbation solution is indistinguishable in Fig. 4 from the numerical solution of the nonlinear system (9)–(11), given by the solid curve.

INITIAL CURVATURE

In this section, the foundation is curved and the beam has initial curvature ($\theta_0 = \beta s$) but the loads have no eccentricity ($\delta = 0$). The initial slope at the support ($s = 1$) is $\alpha = \beta$.

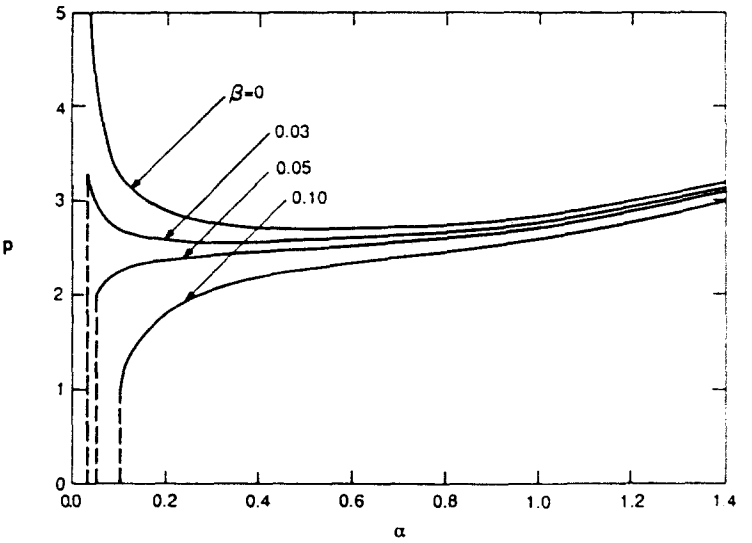

Fig. 5. Effect of initial curvature on load–displacement curves of elastica; $q = 0.1$, $\delta = 0$.

For the shooting method used with eqns (9) and (10), the condition at $s = 1$ is now $\theta'(1) = \beta$. The pressure is taken to be $q = 0.1$. Equilibrium paths in the (α, p) plane are presented in Fig. 5 for $\beta = 0.03$, 0.05 and 0.10, as well as for the perfect system ($\beta = 0$).

As the compressive load is increased, no displacement occurs ($\alpha = \beta$) until a certain threshold is reached. This value is $p = 3.30$, 2.00 and 1.00 for $\beta = 0.03$, 0.05 and 0.10, respectively. If β is sufficiently small, the initial load–displacement curve for $\alpha > \beta$ has a negative slope, e.g. for $\beta = 0.03$ in Fig. 5. For such a case, if p is increased past its threshold value, the elastica suddenly snaps toward an equilibrium state with large displacements. However, if β is sufficiently large, e.g. for $\beta = 0.05$ and 0.10 in Fig. 5, the path is rising and displacements change smoothly with increasing load. Hence buckling only occurs if the initial curvature is sufficiently small.

ECCENTRICITY

Now suppose that the beam is initially straight ($\beta = 0$) but that the loads P are applied quasi-statically at a small distance Δ normal to the centerline and below it. Results for $q = 0.1$ are shown in Fig. 6 with $\delta = 0.01$, 0.02, 0.03, 0.04 and 0.05, along with the concentric case $\delta = 0$. A logarithmic scale is used on the abscissa.

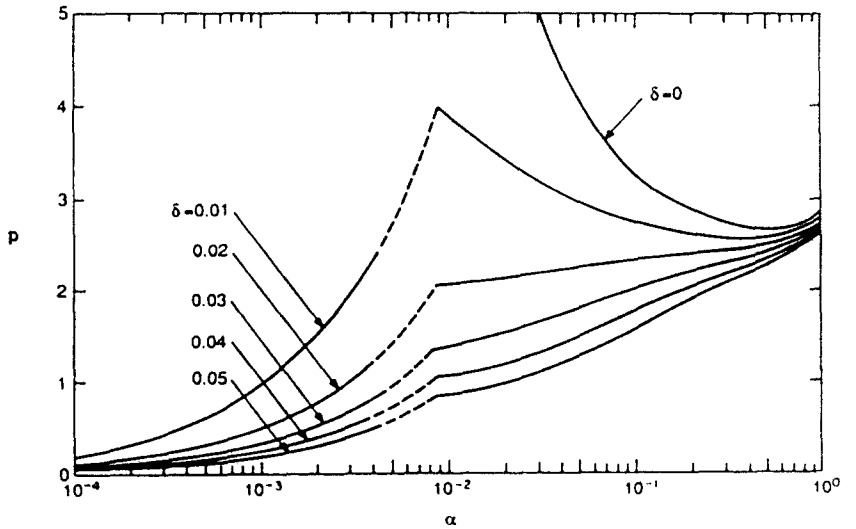

Fig. 6. Effect of eccentricity on load–displacement curves for elastica; $q = 0.1$, $\beta = 0$.

In order to obtain the load–displacement curves in Fig. 6 with $\delta > 0$, first the shooting method was applied to eqns (9) and (10) with $\beta = 0$ and p defined by eqn (11). This yields the solid curves on the right side of the figure. As α is decreased (from $\alpha = 1$), the central deflection of the buckled configuration decreases [see Fig. 7(f), (e), (d)] and reaches zero at the ends of these solid curves [see Fig. 7(c)]. This occurs at $\alpha = 0.009$ and $p = 3.97$, 2.04, 1.37, 1.03 and 0.83 for $\delta = 0.01$, 0.02, 0.03, 0.04 and 0.05, respectively.

For smaller values of α, the beam is constrained by the rigid foundation and the boundary conditions (10) must be altered. In the range where the curves in Fig. 6 are dashed, the beam has no deflection at the centre point ($s = 0$), and the shear force there is not zero [see Fig. 7(c)]. Hence the boundary condition $\theta''(1) = 0$ is replaced by the condition

$$\int_0^1 \sin\theta(s)\,ds = 0 \tag{17}$$

requiring that the deflection be the same at $s = 0$ and $s = 1$. This case will be designated "mode B". For smaller values of α ($\alpha < 0.004$), depicted by solid curves on the left in Fig. 6, the beam has no deflection in a central region [see Fig. 7(a), (b)]. This will be designated "mode A". If lift-off occurs at $s = a$, then the boundary conditions for the buckled section ($a < s < 1$) are given by

$$\theta(a) = 0, \quad \theta'(a) = 0, \quad \theta(1) = 0, \quad \int_a^1 \sin\theta(s)\,ds = 0. \tag{18}$$

For mode A, the rotations are very small. However, since the length of each uplifted section also may be small, the curvature may not be small and the nonlinear term in eqn (9) may be important. Both a nonlinear and a linear analysis were carried out, and it turned out that the results were almost identical. For mode B, a linear solution is also very accurate. The linear solution is presented here, in terms of the beam deflection.

Consider the coordinate $\bar{x}$, measured from the left support, and the upward deflection $\bar{y}$, as shown in Fig. 1(a), and let $y = \bar{y}/L$ and $x = \bar{x}/L$. The linearized equilibrium equation for $y(x)$ is

$$y''''(x) + \gamma^2 y''(x) = -q \tag{19}$$

with the load given by $p = \gamma^2$ and θ related to y by $\theta(x) = -y'(x)$. The solution of eqn (19) has the form

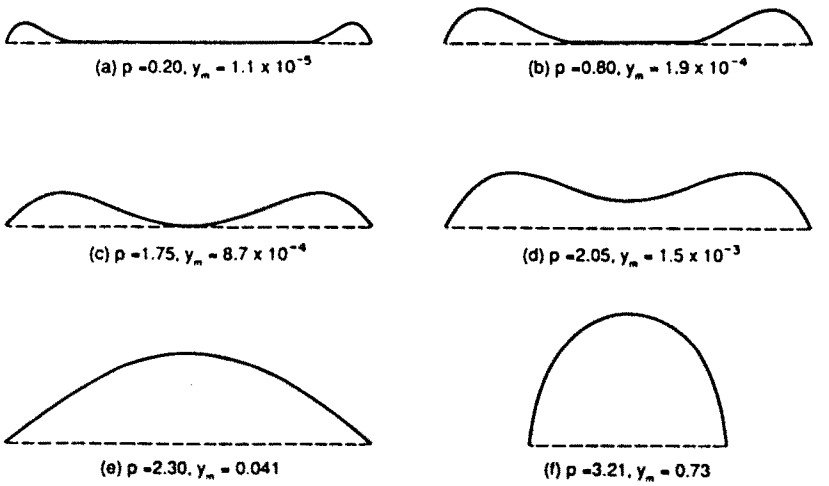

Fig. 7. Buckled configurations of elastica; $q = 0.1$, $\beta = 0$, $\delta = 0.02$. The vertical scales are magnified in (a)–(e).

$$y(x) = -\frac{q}{2\gamma^2}x^2 + d_1 + d_2 x + d_3 \sin \gamma x + d_4 \cos \gamma x. \tag{20}$$

As the eccentric load is increased from zero, the beam first exhibits mode A [Fig. 7(a), (b)]. The nondimensional length of each buckled region is denoted $b (0 < b < 1)$, and the beam has no deflection, rotation or bending moment at $x = b$. Hence the boundary conditions for mode A are

$$y(0) = 0, \quad y''(0) = -p\delta, \quad y(b) = 0, \quad y'(b) = 0, \quad y''(b) = 0. \tag{21}$$

Application of these conditions to eqn (20) leads to a transcendental equation for b and formulae for d_1, d_2, d_3 and d_4, which are given in the Appendix. As mentioned earlier, resulting curves of p as a function of the end rotation α are plotted on the left side of Fig. 6 for five values of eccentricity.

As p is increased, the buckled length b increases. When b reaches unity, mode B takes over [Fig. 7(c)]. In this mode, the bending moment at the center of the beam ($x = 1$) is not zero, so that the boundary conditions are given by the first four conditions in eqn (21) with $b = 1$. The resulting coefficients in eqn (20) are listed in the Appendix, and load–displacement paths are depicted as dashed curves in Fig. 6.

As p is increased further, the dashed curves in Fig. 6 meet the solid equilibrium paths based on eqns (9)–(11), for which the central deflection $y(1)$ is positive [Fig. 7(d), (e), (f)]. Mode B becomes unstable and the center of the beam lifts off the foundation. For eccentricities $\delta = 0.02$, 0.03, 0.04 and 0.05 in Fig. 6, this transition is smooth, since the new equilibrium paths are rising and stable. The sequence of buckling modes for the case $\delta = 0.02$ is illustrated in Fig. 7, where y_m denotes the maximum value of y for each configuration. However, if $\delta \leq 0.01$ and p is increased beyond its bifurcation value $p = 3.97$, the elastica snaps suddenly toward a state with very large displacements. Thus, if the eccentricity is sufficiently small, buckling occurs when the center of the beam first deflects and the curvature of the central region changes sign.

CONCLUDING REMARKS

The work presented here is different in several respects from the studies described in the references. First of all, the ends of the beam considered here are simply supported, whereas the previous investigations treated cases in which the beam is tangential to the foundation at the ends of an uplifted section (usually an interior section of a long beam). Secondly, the case of eccentric loading is included here, but not in the references. In addition, only Wang (1985) also considered downward pressure; the other papers treated a uniformly distributed vertical load (e.g. the weight of the beam). The behavior for these two types of loading is similar when the beam rotations are small.

The foundation profile in the present study is assumed to be flat [Fig. 1(a)] or circular [Fig. 1(b)], with the unstrained beam in full contact with the foundation. [Partial contact is considered, for example, in Richards (1990).] The deflections of the beam turn out to be symmetric about its center. Thus the analysis can be carried out using half of the beam. If the foundation were symmetric but not rigid, asymmetric deflections might occur. The only reference including an asymmetric and rigid foundation is Koh and Quek (1990). In that study, the upheaval buckling loads (corresponding to a jump in the beam configuration as the compressive load is increased) for an asymmetric foundation are sometimes lower and sometimes higher than those for a related symmetric foundation.

In the problem analysed by Yun and Kyriakides (1985), extensibility of the beam had little effect on the results. Here, and in a number of the previous papers, longitudinal deformation is neglected and the beam is assumed to be inextensible. Also, friction between the beam and the foundation is neglected here, although it is included in many of the references.

The forms of the load–displacement curves in Fig. 3 for the flat foundation and Fig. 5 for the circular foundation are similar to those for long, heavy beams, despite the different loading and boundary conditions (e.g. El-Aini, 1975; Hobbs, 1985). For the initially-curved beam, no deflection occurs until the compressive load reaches a certain value, and then the system may buckle (if the initial curvature is sufficiently small) or deform smoothly. If the beam is initially flat and the load is applied eccentrically below the beam centerline, uplifting begins at the ends and extends as the load is increased (Fig. 7). If the eccentricity is sufficiently small (e.g. if $\delta = 0.01$ in Fig. 6), buckling occurs as the load is increased past a certain value.

Acknowledgements—The authors are grateful to C.-C. Cheng for carrying out the numerical computations. They also acknowledge helpful suggestions by the reviewers.

REFERENCES

Ariman, T. (1983). A review of buckling and rupture failures in pipelines due to large ground deformations. In *Earthquake Behavior and Safety of Oil and Gas Storage Facilities, Buried Pipelines and Equipment* (Edited by T. Ariman), PVP-Vol. 77, pp. 176–180. ASME, New York.

Courbon, J. (1980). The equilibrium of a heated beam resting over a rigid horizontal plane (in French). *J. Mec. Appliq.* **4**, 385–406.

El-Aini, Y. M. (1975). A nonlinear analysis for one-way buckling of a laterally loaded column. *J. Mech. Engng Sci.* **17**, 150–154.

El-Aini, Y. M. (1976). Effect of foundation stiffness on track buckling. *J. Engng Mech. Div. ASCE* **102**, 531–545.

Friedmann, Y. (1989). In-service mechanical behavior of heated pipelines laid on seabed surface. In *Proc. 8th Int. Conf. on Offshore Mech. and Arctic Engng* (Edited by J. S. Chung, K. Karal, T. Taira and S. T. Barbas), Vol. V, pp. 113–119. ASME, New York.

Hobbs, R. E. (1981). Pipeline buckling caused by axial loads. *J. Construc. Steel Res.* **1**, 2–10.

Hobbs, R. E. (1984). In-service buckling of heated pipelines. *J. Transp. Engng* **110**, 175–189.

Hobbs, R. E. (1985). Discussion of: Buckling and postbuckling of the lying sheet (by C. Y. Wang). *Int. J. Solids Structures* **21**, 423–424.

Hobbs, R. E. (1989). Two-dimensional upheaval buckling of a heavy sheet. *Thin-Walled Struc.* **8**, 235–252.

Hobbs, R. E. (1990). Axisymmetric upheaval buckling of a heavy sheet. *J. Appl. Mech.* **57**, 472–474.

Hobbs, R. E. and Liang, R. (1989). Thermal buckling of pipelines close to restraints. In *Proc. 8th Int. Conf. on Offshore Mech. Arctic Engng* (Edited by J. S. Chung, K. Karal, T. Taira and S. T. Barbas), Vol. V, pp. 121–127. ASME, New York.

Ju, G. T. and Kyriakides, S. (1988). Thermal buckling of offshore pipelines. *J. Offshore Mech. Arctic Engng* **110**, 355–364.

Kerr, A. D. (1973). A model study for vertical track buckling. *High Speed Ground Transp. Jl* **7**, 351–368.

Kerr, A. D. (1974). On the stability of the railroad track in the vertical plane. *Rail Int.* **2**, 131–142.

Kerr, A. D. (1976). The effect of lateral resistance on track buckling analyses. *Rail Int.* **1**, 30–38.

Kerr, A. D. (1978a). Analysis of thermal track buckling in the lateral plane. *Acta Mech.* **30**, 17–50.

Kerr, A. D. (1978b). Lateral buckling of railroad tracks due to constrained thermal expansions—a critical survey. In *Railroad Track Mechanics and Technology* (Edited by A. D. Kerr), pp. 141–169. Pergamon Press, Oxford.

Kerr, A. D. (1979). On thermal buckling of straight railroad tracks and the effect of track length on the track response. *Rail Int.* **9**, 759–768.

Kerr, A. D. (1980). An improved analysis for thermal track buckling. *Int. J. Non-Lin. Mech.* **15**, 99–114.

Kerr, A. D. (1989). Additional comments on buckling analyses of embedded layers. *Tectonophys.* **169**, 149–152.

Koh, C. G. and Quek, S. T. (1990). Limit loads of buried pipelines with asymmetric initial imperfections. *J. Pres. Ves. Tech.* **112**, 392–396.

Kyriakides, S., Yun, H. D. and Yew, C. H. (1983). Buckling of buried pipelines due to large ground movements. In *Earthquake Behavior and Safety of Oil and Gas Storage Facilities, Buried Pipelines and Equipment* (Edited by T. Ariman), PVP-Vol. 77, pp. 140–150. ASME, New York.

Love, A. E. H. (1944). *A Mathematical Treatise on the Theory of Elasticity* (4th Edn). Dover, New York.

Mróz, Z. and Plaut, R. H. (1992). On the stability and post-critical behavior of elastic structures with dry friction. *Int. J. Solids Structures* **29**(10), 1241–1253.

Nielsen, N. J. R., Lyngberg, B. and Pedersen, P. T. (1990). Upheaval buckling failures of insulated buried pipelines: a case story. In *Proc. 22nd Annual Offshore Tech. Conf.*, pp. 581–592, Houston.

Nielsen, N. J. R., Pedersen, P. T., Grundy, A. K. and Lyngberg, B. S. (1988). New design criteria for upheaval creep of buried subsea pipelines. In *Proc. 7th Int. Conf. Offshore Mech. Arctic Engng*, Vol. V, pp. 243–249. ASME, New York.

Pedersen, P. T. and Jensen, J. J. (1988). Upheaval creep of buried heated pipelines with initial imperfections. *Marine Struc.* **1**, 11–22.

Pedersen, P. T. and Michelsen, J. (1988). Large deflection upheaval buckling of marine pipelines. In *Proc. 4th Int. Conf. Behaviour of Offshore Struc.*, Vol. 3, pp. 965–980. Trondheim, Norway.

Richards, D. M. (1990). The effect of imperfection shape on upheaval buckling behavior. In *Advances in Subsea Pipeline Engineering and Technology* (Edited by C. P. Ellinas), pp. 51–66. Kluwer, Dordrecht.

Roorda, J. (1988). Buckles, bulges, and blow-ups. In *Applied Solid Mechanics—2* (Edited by A. S. Tooth and J. Spence), pp. 347–380. Elsevier, London.

Samavedam, G., Kish, A., Thurston, M. and Jeong, D. (1988). Recent advances in track buckling mechanics. In *Applied Mechanics Rail Transportation Symposium—1988* (Edited by V. T. Hawthorne, E. H. Law and P. Tong), AMD-Vol. 96, RTD-Vol. 2, pp. 95–100. ASME, New York.

Taylor, N. and Gan, A. B. (1986). Submarine pipeline buckling—imperfection studies. *Thin-Walled Struc.* **4**, 295–323.
Tvergaard, V. and Needleman, A. (1981). On localized thermal track buckling. *Int. J. Mech. Sci.* **23**, 577–587.
Vinogradov, A. M. (1988). Buckling analysis of pipelines supported by soil media. In *Elastic–Plastic Failure Modelling of Structures with Applications* (Edited by D. Hui and T. J. Kozik), PVP-Vol. 141, pp. 89–96. ASME, New York.
Wang, C. Y. (1984). On symmetric buckling of a finite flat-lying heavy sheet. *J. Appl. Mech.* **51**, 278–282.
Wang, C. Y. (1985). Post-buckling of a pressurized elastic sheet on a rigid surface. *Int. J. Mech. Sci.* **27**, 703–709.
Wang, C. Y. (1986). A critical review of the heavy elastica. *Int. J. Mech. Sci.* **28**, 549–559.
Yun, H. and Kyriakides, S. (1985). Model for beam-mode buckling of buried pipelines. *J. Engng Mech.* **111**, 235–253.
Yun, H. D. and Kyriakides, S. (1986). Buckling of pipelines in seismic environments. In *Proc. 3rd U.S. Nat. Conf. on Earthquake Engng*, Vol. III, pp. 2179–2189. Charleston, South Carolina.
Yun, H. D. and Kyriakides, S. (1988). Localized plastic buckling of a heavy beam on a contacting surface. *J. Pres. Ves. Tech.* **108**, 146–150.
Yun, H. and Kyriakides, S. (1990). On the beam and shell modes of buckling of buried pipelines. *Int. J. Soil Dyn. Earthquake Engng* **9**, 179–192.

APPENDIX

In eqn (16),

$$c_1 = -\frac{\gamma_1^2 r}{\gamma_1^4} - \frac{r^3}{2\gamma_1^8} - \frac{3r^3}{4\gamma_1^8\cos^2\gamma_1}, \quad c_2 = \frac{\gamma_1^2 r}{2\gamma_1^6\cos\gamma_1} + \frac{3r^3}{4\gamma_1^9\cos\gamma_1} + \frac{3r^3}{16\gamma_1^9\cos^3\gamma_1}, \quad c_3 = \frac{r^3}{8\gamma_1^9\cos^2\gamma_1},$$

$$c_4 = -\frac{r^3}{192\gamma_1^9\cos^4\gamma_1},$$

where

$$\gamma_1^2 = \frac{r^2[12\gamma_1\sin\gamma_1(1+4\cos^2\gamma_1) - \cos\gamma_1(61+4\cos^2\gamma_1)]}{32\gamma_1^4\cos^4\gamma_1(2-\gamma_1\tan\gamma_1)}$$

For mode A of the elastica, the buckled length b is a root of the equation

$$2b(\gamma^4\delta - q + q\cos\gamma b) + \gamma(qb^2 - 2\gamma^2\delta)\sin\gamma b = 0$$

and the coefficients in eqn (20) are

$$d_1 = (q-\gamma^4\delta)/\gamma^4, \quad d_2 = \frac{\gamma^4\delta + q(\gamma b\sin\gamma b + \cos\gamma b - 1)}{\gamma^3\sin\gamma b}, \quad d_3 = \frac{(q-\gamma^4\delta)\cos\gamma b - q}{\gamma^4\sin\gamma b}, \quad d_4 = (\gamma^4\delta - q)/\gamma^4.$$

For mode B, the coefficients d_1 and d_4 are the same as for mode A, and

$$d_2 = \frac{q\gamma(\gamma\cos\gamma - 2\sin\gamma) + 2(\gamma^4\delta - q)(\cos\gamma - 1)}{2\gamma^3(\gamma\cos\gamma - \sin\gamma)}, \quad d_3 = \frac{q\gamma^2 + 2(\gamma^4\delta - q)(\gamma\sin\gamma + \cos\gamma - 1)}{2\gamma^4(\gamma\cos\gamma - \sin\gamma)}.$$